



Altered Electroencephalography Microstates During the Motor Preparation Process for Voluntary and Instructed Action

Lipeng Zhang,^{1,2} Tongda Shen,³ Rui Zhang^{1,2} and Yuxia Hu^{1,2,*}

Abstract

There is an urgent need to identify biomarkers of the motor preparation process in cognitive neuroscience. In this study, voluntary and instructed action experimental paradigms were designed and 29 participants were recruited. The electroencephalography (EEG) microstate analysis method was used to calculate the occurrence, duration, coverage, and transition probabilities of microstates for resting state, voluntary, and instructed conditions, as well as left-hand (LH) and right-hand (RH) movement conditions. We found significantly higher occurrence and coverage of microstate A in the motor preparation stage of instructed and voluntary conditions compared to the resting state. However, the occurrence, duration, and coverage of microstates between instructed and voluntary conditions did not show a significant difference. Furthermore, the occurrence, duration, and coverage of microstate A were significantly higher for the left hand compared to the right hand. In addition, the occurrence, duration, and coverage of microstate B were significantly higher for the right hand compared to the left hand. Our results demonstrated alterations in the parameters of EEG microstates between the resting state and motor preparation. We also observed significant differences between left- and right-hand movements. These findings could help us understand the neural mechanism of motor preparation based on the whole-brain network.

Keywords: EEG microstates; Motor preparation; Voluntary action; Instructed action; Resting-state; Left/right-hand movement.

Received: 04 January 2022; Revised: 07 February 2022; Accepted: 10 February 2022.

Article type: Research article.

1. Introduction

Understanding how the brain functions before action is an important topic in neuroscience. In general, actions triggered by internal neuronal activity in the brain are defined as voluntary,^[1,2] while those induced by external cues are considered to be instructed. In 1965, Kornhuber *et al.* described slow-rising negative electrical activity that started about 2 s before voluntary action and was called the readiness potential (RP).^[3] Some studies also found the presence of RP before instructed action.^[4,5] However, the distribution of RP before voluntary action was more anterior^[5-7] compared to that before instructed action. In addition, several neuroimaging studies have shown that voluntary and instructed actions have similar activations of supplementary and cingulate motor

areas.^[8-11] Some studies also reported that the mechanisms underlying motor preparation and imagery are similar, thus event-related desynchronization (ERD) may occur in the sensorimotor areas during motor preparation.^[12-14]

The brain networks need to work together and require rapid switching between different modes to perform upcoming tasks.^[15-18] Multichannel electroencephalography (EEG) microstates are a well-established method for characterizing the spatiotemporal features of large-scale brain activity.^[19] This method has been extensively used to investigate resting-state EEG data, and four canonical microstate maps were identified by applying the agglomerative clustering procedure.^[20,21] With simultaneous EEG-fMRI technology, some studies have found that EEG microstates are closely related to resting-state networks.^[22-24] Numerous studies confirmed that the EEG microstate could be modulated by diseases such as schizophrenia,^[25,26] disorders of consciousness,^[27] and dementia.^[28-29,30]

Previous studies of the motor preparation process mainly focused on the readiness potential.^[31] However, whether RP reflects the motor preparation process is controversial.^[32] If the microstates are altered during motor preparation, it would

¹ School of Electrical Engineering, Zhengzhou University, Zhengzhou 450001, China.

² Henan Key Laboratory of Brain Science and Brain-Computer Interface Technology, Zhengzhou 450001, China.

³ Tandon School of Engineering of New York University, New York, USA.

*Email: huyuxia@zzu.edu.cn (Y. Hu)

suggest the state of the brain has changed before motor activity. This change may help us to explain the mechanism of the motor preparation process. Besides, the microstate differences between left and right-hand movements during motor preparation have not been explored until now. Thus, this paper mainly studies the following two questions. Firstly, whether the microstates' switching modes altered during the motor preparation phase of voluntary and instructed action compared to the resting state. Secondly, whether the switching modes also changed between left and right-hand movement for voluntary and instructed action.

The aim of the present study was to explore the spatiotemporal characterization of the EEG microstates during motor preparation. First, the experimental paradigms of voluntary and instructed actions were designed. During the experiment, participants were asked to complete left-hand and right-hand movement tasks, and the EEG data were obtained. Then, according to the resting state, voluntary, and instructed conditions, the EEG data were grouped and preprocessed. Similar operations were done according to left and right-hand movements for voluntary and instructed action. Finally, occurrence, duration, coverage, and transition probabilities were analyzed for all groups.

2. Methods

2.1 Participants

Twenty-nine participants (average age: 26.5 ± 2 years; eight females; all right-handed) from Zhengzhou University, China, were included in the experiment. All participants had the normal or corrected-to-normal vision, and none had motor or neurological disease. The participants gave written informed consent and the study followed the Declaration of Helsinki.

2.2 Design of the experimental paradigm

To investigate the alterations in brain EEG microstates between the resting state and motor preparation stage for voluntary and instructed actions, two experiments were conducted. During these experiments, we recorded the electromyography (EMG) signals from the left and right hands to identify the onset of movements and distinguish the movements of the left and right hands. The participant's hand was placed on the armrest of the chair. Gently lift the left or right hand according to the experimental task, and then lower it.

2.2.1 Experiment 1: Instructed action paradigm

At the beginning of each trial, a cross appeared in the center of the screen (Fig. 1a). During the next 3 s, participants were asked not to move their hands, forearms, or elbows from the chair armrests. Next, a green line with an arrow (left or right) was presented in the center of the screen for 0.5 s. When the cue disappeared, participants prepared for the tasks instructed by the visual clue (left-pointing arrow referred to left-hand movement, LH; right-pointing arrow referred to right-hand movement, RH). After a delay of approximately 2 s, the

participants performed corresponding hand movements. Then, 5 s after the visual clue, an auditory cue informed the participants that the trial was over. During each run, LH and RH tasks were randomly presented. The interval between the neighboring trials was 2.5–3.5 s. Thirty trials (15 trials each for the LH and RH tasks) were included in a single run. Ten runs were completed for each participant. The duration of each run was about 4 minutes and there was 3 minutes break between consecutive runs.

2.2.2 Experiment 2: Voluntary action paradigm

In experiment 2, participants performed LH and RH tasks according to their will, with no instructed clues being presented on the screen. At the beginning of each run (Fig. 1b), the participants were asked to remain still. After the examiner informed the participant that the LH/RH task could be started, the participants were allowed to perform hand movements at their own will. In each trial, the participants automatically stopped after completing the task. The participants were asked to complete only one hand movement for each trial. To avoid overlap between two trials, the participants were reminded to control the time interval of adjacent trials to > 8 s before each run. But, participants did not need to count for time estimation. We would remove trials with time intervals less than 8s in the later EEG data processing. Each run lasted about 5 min. Each run included about 30 trials. LH and RH tasks were divided almost equally. Ten runs were conducted for each participant. Compared to the instructed movements, voluntary movements were internally generated endogenous actions.

2.2.3 EEG recording

The experiment was completed in a magnetically shielded room with normal light and temperature. Each participant was seated in a comfortable chair. The participant's eyes and the center of the screen were at the same height, and he/she was asked to focus on the center point of the screen. The screen was placed almost 80 cm away from the participants. During data recording, participants were asked to avoid eyeball movements, swallowing, and unnecessary limb movements.

2.2.4 Experimental setup

Raw EEG data were recorded using the Neuroscan NuAmps digital amplifier system with 64-electrode DC-EEG recording arranged in the standard 10–20 EEG configuration. The selected 59 EEG electrodes and their positions are shown in Fig. 1d. These electrodes covered all brain regions. Horizontal and vertical electrooculograms (HEOG and VEOG) were also recorded using bipolar montages with electrodes placed on the left and right external canthi, and above and below the left eye. We used two extended bipolar channels (BP3 and BP4), which consisted of two electrodes (one was a reference electrode, Fig. 1c), to acquire the left and right arm EMG data. The EEG data were obtained at a sampling rate of 250 Hz, and the impedance of all electrodes was < 5 K Ω . The reference electrode was placed between the Cz and CPZ electrodes. The

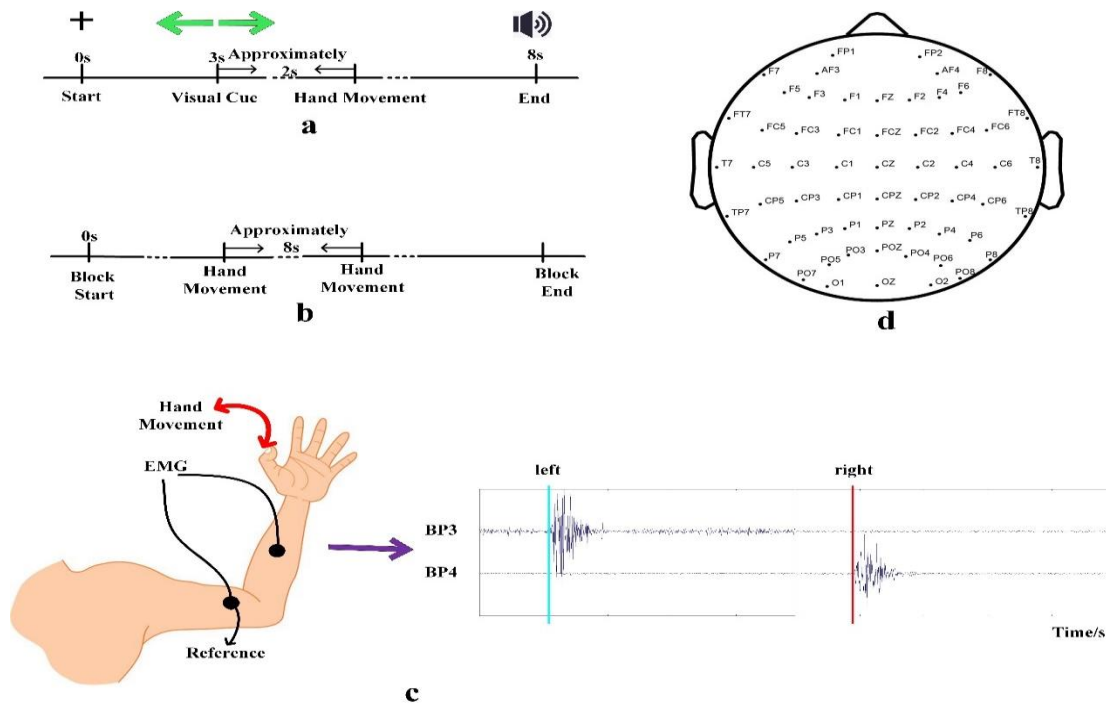


Fig. 1 (a) Procedure of experiment 1. (b) Procedure of experiment 2. (c) Schematic diagram showing the positions of EMG electrodes and action onset detection. (d) Locations of selected 59 electrodes.

experiment program was implemented using the E-Prime 2.0 software.

2.3 Data processing

2.3.1 EMG analysis

The hand movement onset time was identified from the EMG data.^[33] First, the EMG data were filtered using a zero-phase shift bandpass filter with cutoff frequencies of 6 and 50 Hz. Then, the power of the filtered data was calculated, and the thresholds to detect the onset time of action were set (Fig. 1c). There were two thresholds used to detect the movement onset. The first threshold was used for coarse selection. It was used to distinguish between real movement and noise. The second threshold was used to detect movement onset based on the results of the former threshold. Usually, the first and second thresholds were set to 10 and 3 times the EMG average energy. Finally, the onset times were saved as a TXT file for further analysis.

2.3.2 EEG signal preprocessing

First, the polluted segments were manually rejected, and bad channels were replaced with the mean of surrounding electrodes. Then, eye movements, EMG, and electrocardiograph (ECG) artifacts were removed by independent component analysis.^[34] The cleaned EEG data were re-referenced to the common average reference.^[35] With a zero-phase shift filter, the re-referenced data were filtered through a 2–40 Hz band pass filter. To assess changes in EEG microstates at resting state and during voluntary and instructed movements, continuous data were divided into epochs. For the resting state, we extracted epochs in the $[-4.1, -2]$ s interval

before the EMG onset of voluntary action with a baseline of $[-4.1, -4]$ s. For voluntary and instructed conditions, the epochs in the $[-2.1, 0]$ s of voluntary and instructed actions were extracted with a baseline of $[-2.1, -2]$ s. In the current study, LH and RH tasks were extracted separately. However, the LH and RH epochs were merged during analysis to detect the differences between the resting state, voluntary, and instructed conditions. These cleaned epochs were imported to the Microstate EEGlab toolbox for further analysis.^[36]

2.3.3 EEG microstate analysis

Microstate analysis mainly consisted of the following steps.^[19] First, the global field power (GFP) of the cleaned epochs was calculated. GFP is a measure of the strength of global activation. To obtain accurate results, 2,000 GFP peaks were randomly selected and these EEG points were extracted for cluster analysis. Second, the modified K-means algorithm, which ignores the polarity of the EEG topography, was utilized to identify the microstates. To obtain comparable results, the number of clusters was set to four, and four microstate classes were obtained for each condition. Then, individual EEG epochs were fitted back with the four generated microstate classes. Finally, the following microstate parameters for each microstate segmentation class were calculated as follows.

- (a) Occurrence: the average number of times per second a microstate is dominant.
- (b) Duration: the average duration of a given microstate.
- (c) Coverage: the fraction of time a given microstate is active.
- (d) Transition probabilities: a measure of how frequently microstates of a certain class are followed by microstates of other classes.

2.3.4 Statistical analysis

For the first question, there was one independent variable (three levels: resting state, voluntary and instructed conditions) and four dependent variables (microstate A, B, C, and D). Hence, we designed a one-way multivariate analysis of variance (MANOVA). If there was a significant difference, we designed ANOVA to detect differences among the three conditions for each microstate's parameters (occurrence, duration, and coverage). Then, post hoc multiple comparisons were performed to detect the differences between any two conditions. Finally, we analyzed the differences in the transition matrices between resting state and voluntary conditions with a two-sample t-test method. The same statistical analysis method was performed between the resting state and instructed conditions.

For the second question, since there were only LH and RH conditions, two-sample t-tests were used to test the differences in each microstate's parameters. To correct for multiple comparisons, we applied the Benjamini and Hochberg false discovery rate correction method for the two-sample t-test method.^[37] All statistical analyses were performed using MATLAB.

3. Results

To obtain a balanced cross-validation criterion (CV) and global explained variance (GEV),^[38] four clusters across the conditions were obtained. According to the topography of the

four microstate maps, we sorted these into microstates A, B, C, and D. Microstate A showed left occipital to right frontal orientation; microstate B showed left frontal to right occipital orientation; microstate C showed frontal-temporal to occipital orientation, and microstate D showed central frontal to occipital orientation. The topography of the four microstate classes was similar to that in a previous study.^[19]

3.1 EEG microstates during resting state, voluntary, and instructed conditions

Figure 2a shows the four canonical EEG microstates for resting state, voluntary, and instructed conditions. The GEV of the four EEG microstates were 61.6%, 62.4%, and 63.2% for the aforementioned three conditions, respectively. The values of GEV were similar to those reported in previous studies of EEG microstates.^[22,39] The results of MANOVA show that there were significant differences ($p < 0.05$) among the three conditions for each microstate's parameters. The results of ANOVA show that there were significant differences in the parameters of microstate A. Fig. 2b–d shows the occurrence, duration, and coverage of the microstate parameters of the aforementioned three conditions. Compared to the resting state, the occurrence of microstate A was significantly higher under voluntary ($p < 0.01$) and instructed ($p < 0.05$) conditions. Similar results were obtained for the coverage of microstate A. The parameters of microstates B–D did not show significant differences from those of the resting state. Fig. 2e

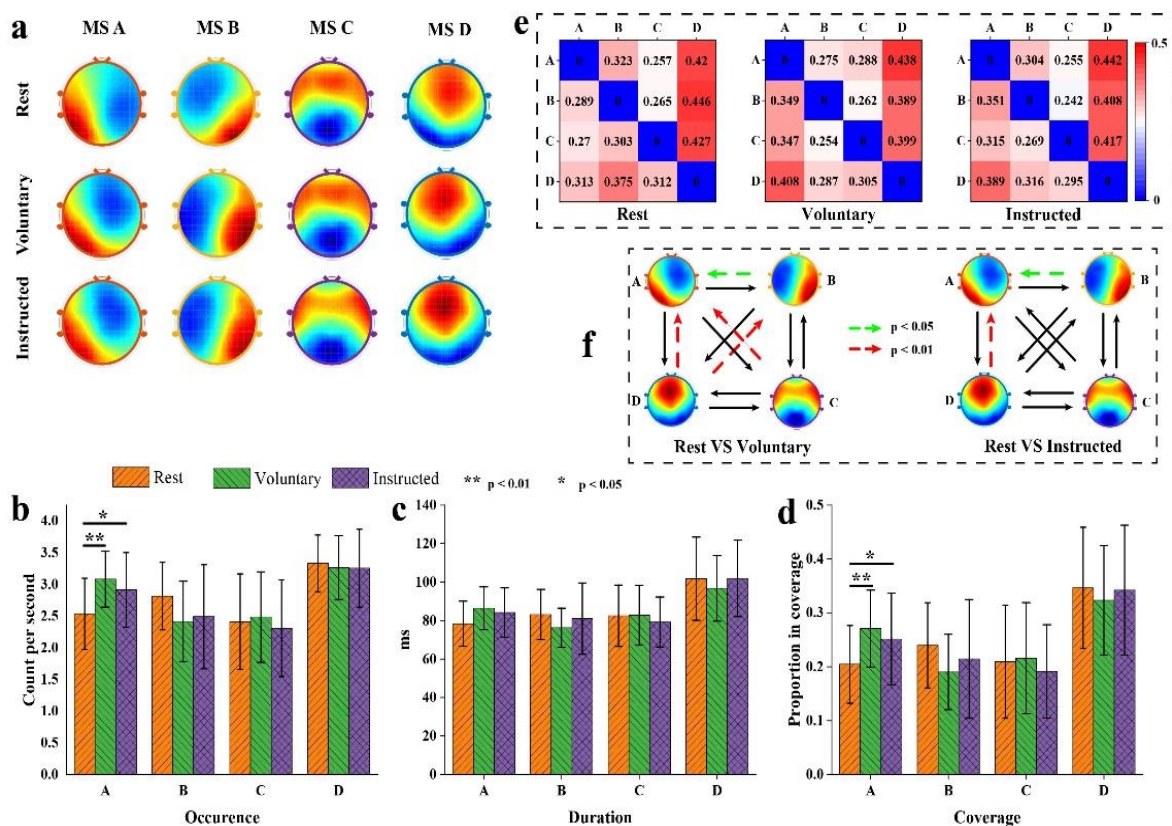


Fig. 2 EEG microstates during resting state, voluntary, and instructed action conditions. a) EEG microstate classes, b) occurrence, c) duration, d) coverage, and e, f) transition probabilities. (* or green arrows denote $p < 0.05$, ** or red arrows denote $p < 0.01$, and error bars represent the standard error).

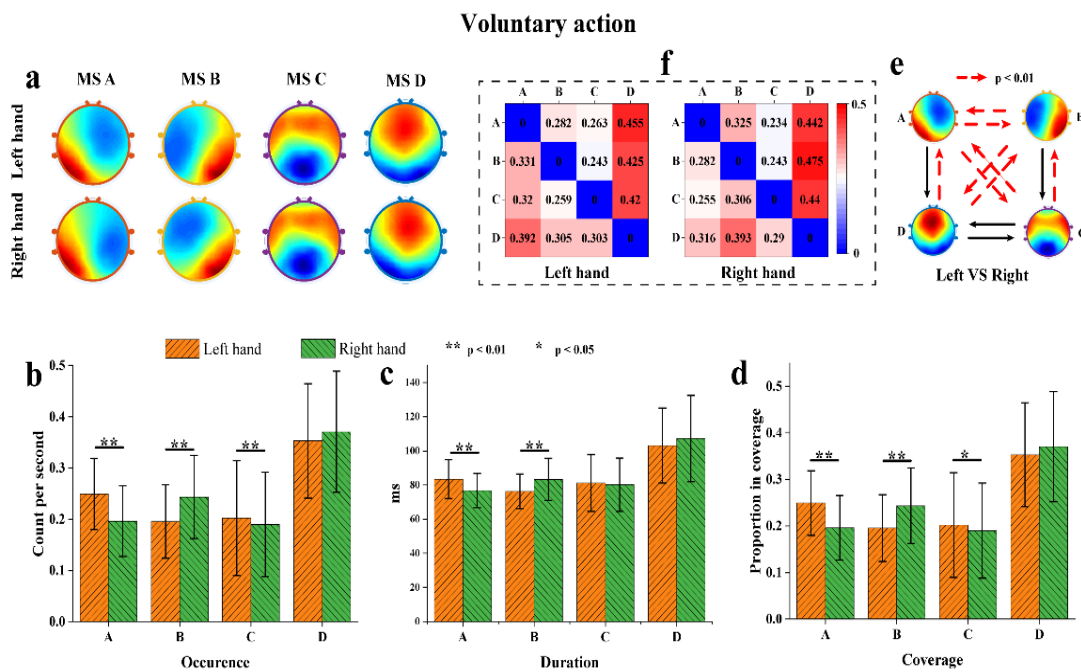


Fig. 3 EEG microstates during voluntary action in the LH and RH conditions. a) EEG microstate classes, b) occurrence, c) duration, d) coverage, and e, f) transition probabilities. (*denotes $p < 0.05$, ** or red arrow denote $p < 0.01$, error bars represent the standard error).

and f show the ground average transition among microstates of the three conditions. Statistical analysis of the transition probabilities of conditions revealed significant differences in the four transitions (Tr) for resting-state vs. voluntary conditions: Tr ($B \rightarrow A$, $p < 0.05$), Tr ($C \rightarrow A$, $p < 0.01$), Tr ($D \rightarrow A$, $p < 0.01$), and Tr ($D \rightarrow B$, $p < 0.01$). For the resting state vs. voluntary conditions, we observed a significant difference in the two transitions: Tr ($B \rightarrow A$, $p < 0.01$) and Tr ($D \rightarrow A$, $p < 0.01$).

3.2 EEG microstates under LH and RH conditions for voluntary action

Figure 3a shows the four canonical EEG microstates under LH and RH conditions during voluntary action. The GEV of the four EEG microstates was 62.4% and 62.3% for the aforementioned two conditions, respectively. The topology of the EEG microstates showed that the right frontal area of microstate A had greater neural activity during the LH condition compared to the RH condition. However, the left frontal area of microstate B showed more obvious neural activity during the RH condition compared to the LH condition. Microstates C and D were similar between the two conditions. Fig. 3b–d shows the occurrence, duration, and coverage of the LH and RH conditions. The occurrence, duration, and coverage of microstate A were significantly higher in the LH condition compared to the RH condition ($p < 0.01$), whereas those of microstate B were significantly higher in the RH condition compared to the LH condition ($p < 0.01$). The occurrence and coverage of microstate C were significantly higher in the LH condition compared to the RH condition ($p < 0.01$ and $p < 0.05$, respectively). Fig. 3e and f

show the ground average transition among microstates for the two conditions. Statistical analysis of the transition probabilities of conditions revealed significant differences in eight transitions (Tr) for LH vs. RH condition: Tr ($B \rightarrow A$, $p < 0.01$), Tr ($C \rightarrow A$, $p < 0.01$), Tr ($D \rightarrow A$, $p < 0.01$), Tr ($A \rightarrow B$, $p < 0.01$), Tr ($C \rightarrow B$, $p < 0.01$), Tr ($D \rightarrow B$, $p < 0.01$), Tr ($A \rightarrow C$, $p < 0.01$), and Tr ($B \rightarrow D$, $p < 0.01$).

3.3 EEG microstates during LH and RH conditions for instructed action

Figure 4a shows the four canonical EEG microstates for LH and RH conditions during instructed action. The GEV of the four EEG microstates was 63.2% and 63.1% for the LH and RH conditions, respectively. Similar to the voluntary action, the right frontal area of microstate A showed more obvious neural activity during the LH condition compared to the RH condition. However, the left frontal area of microstate B showed more obvious neural activity in the RH condition compared to the LH condition. Microstates C and D did not show significant differences between the two conditions. Fig. 4b–d shows the occurrence, duration, and coverage of the two conditions. The occurrence, duration, and coverage of microstates A and C were significantly higher in the LH condition compared to the RH condition ($p < 0.01$). The occurrence of microstate B was significantly higher in the RH condition compared to the LH condition ($p < 0.05$). The coverage of microstate D was also significantly higher in the RH condition compared to the LH condition ($p < 0.01$). Fig. 4e and f show the ground average transition among the microstates for the two conditions. Statistical analysis of the transition probabilities of conditions revealed significant

differences in all transitions (Tr) in the

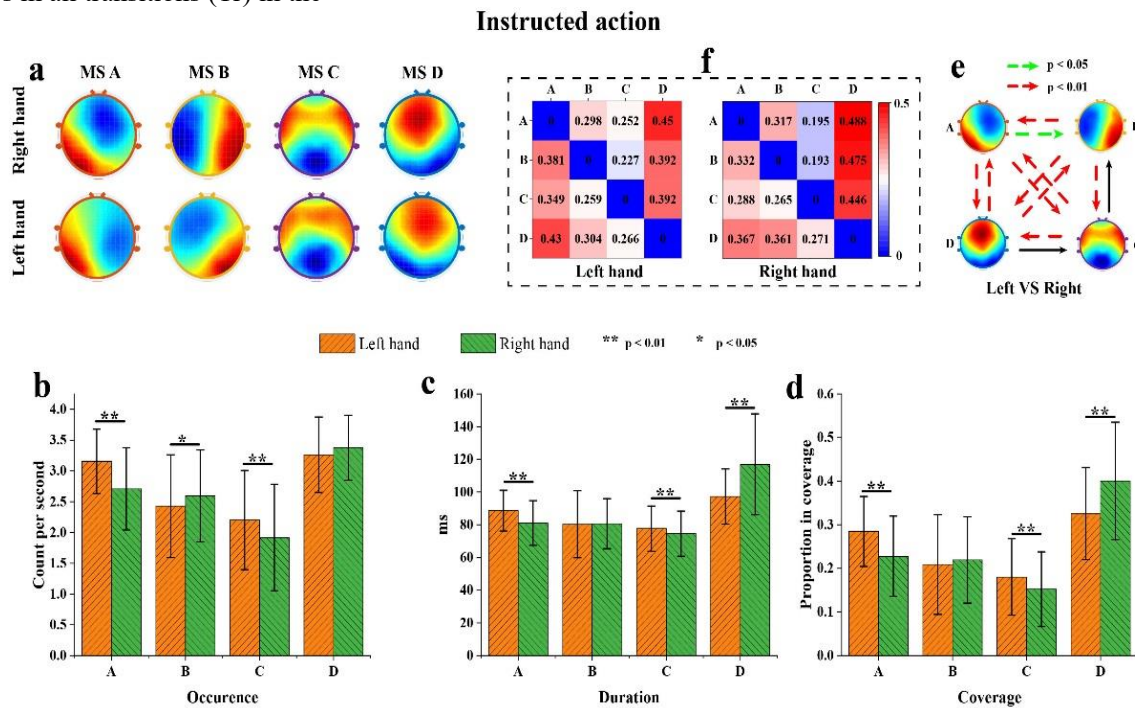


Fig. 4 EEG microstates during instructed action in the LH and RH conditions. a) EEG microstate classes, b) occurrence, c) duration, d) coverage, and e, f) transition probabilities. (* or green arrow denote $p < 0.05$, ** or red arrow denote $p < 0.01$, error bars represent the standard error).

LH vs. RH condition, except for $Tr(D \rightarrow C)$ and $Tr(C \rightarrow B)$.

4. Discussion

The present study investigated changes in large-scale network interactions during motor preparation phases under different conditions based on EEG microstates. We found that compared to the resting state, the occurrence and coverage of microstate A were significantly higher during the motor preparation stage. In addition, under LH and RH conditions of voluntary action, the occurrence, duration, and coverage of microstate A were significantly higher for LH compared to RH. The occurrence, duration, and coverage of microstate B were significantly higher for the RH condition compared to the LH condition. The results of instructed action in the LH and RH conditions were similar to those for voluntary action, except for the significant increase in microstate D during the RH condition compared to the LH condition.

Previous studies have demonstrated that EEG microstates represent large spatial-scale cortical neuronal activities of the cerebral cortex.^[19,40] Compared to the resting-state condition, the occurrence and coverage of microstate A showed significant differences during voluntary and instructed action conditions. Distinct neural pathways for the voluntary and instructed action (*i.e.*, lateral and medial pathways) have been identified.^[41] No significant difference was observed between voluntary and instructed action. According to previous studies of EEG and fMRI, microstates A, B, C, and D correlate to the auditory, visual, saliency, and attention networks.^[19,22] Microstate A is associated with low-level sensory areas,^[27]

therefore the increase in the occurrence and coverage of microstate A before movement may be related to the sensory input of the motor preparation process. However, the high-level cognitive neural networks—microstates C and D—did not show significant differences. One possible reason is that the movement task does not require high-level cognitive attention. Similarly, the microstate parameters did not show significant differences between voluntary and instructed conditions. Generally, the instructed action involves a more complex cognitive circuit,^[42] which may be attributable to the simple information included in the cues in the present study.

Comparisons between the resting state and voluntary conditions revealed that four out of the 12 connections have significant differences in transition probabilities. Specifically, the voluntary condition has a higher transition probability for $Tr(B \rightarrow A)$, $Tr(C \rightarrow A)$, and $Tr(D \rightarrow A)$, but a lower transition probability for $Tr(D \rightarrow B)$. For resting state and instructed conditions, two out of the 12 connections showed significant differences in transition probabilities. The instructed condition had a higher transition probability for $Tr(B \rightarrow A)$ and $Tr(D \rightarrow A)$. As mentioned previously, microstate A is related to low-level sensory areas and a higher transition probability indicates greater sensory input processing tasks.

During voluntary action, the occurrence, duration, and coverage of microstate A significantly higher in the LH condition compared to the RH condition. In addition, the occurrence, duration, and coverage of microstate B were significantly higher in the RH condition compared to the LH condition. Because the LH and RH conditions require the

higher activity of low-level sensory areas, we cannot interpret this as a difference in the auditory or visual network.^[19] After careful observation of the topology of microstates, the right frontal area of microstate A showed more obvious neural activity in the LH condition compared to the RH condition. However, the left frontal area of microstate B exhibited more obvious neural activity in the RH condition compared to the LH condition. The topology of microstates A and B may be influenced by ERD during movement preparation.^[43] The ERDs over the contralateral motor cortex lead to changes in the topology and parameters of microstates A and B. In addition, compared to the RH condition, the occurrence and coverage of microstate C were significantly higher in the LH condition. Microstate C is related to the anterior insula (AI) and dorsal anterior cingulate cortex (dACC),^[44,45] and belongs to a high-level cognitive neural network. During movement, AI is related to sensory evidence accumulation^[6,8] and ACC is related to the sustained pre-movement activity.^[46] However, we believe that these changes may be due to the fact that all participants in this study were right-handed. LH movements are more complex than RH movements.^[47] This phenomenon may also be interpreted as left-brain dominance for motor planning in humans.^[48]

About eight out of the 12 connections showed significant differences in transition probabilities in the LH/RH condition during the voluntary condition. In particular, the LH condition had a higher transition probability during Tr (B → A), Tr (C → A), Tr (D → A), and Tr (A → C), but a lower transition probability for Tr (A → B), Tr (C → B), Tr (D → B), and Tr (B → D) compared to the RH condition. For the LH condition, the transition probability from B, C, and D to A was significantly higher. For the RH condition, the transition probability from A, C, and D to B was significantly higher. These results coincide with the observed changes in microstate parameters.

The results were similar between the instructed and voluntary conditions, except for the significant increase in microstate D during the RH condition compared to the LH condition. Microstate D is mainly produced by frontal-parietal cortices and is related to the attention network.^[19,29] Our results show that the instructed RH movement relies more on the attention network than the instructed LH movement.

In this paper, we studied the EEG microstates during the motor preparation process for voluntary and instructed action. This is a preliminary study. Our results demonstrated alterations in the parameters of EEG microstates between the resting state and motor preparation. We also observed significant differences between left- and right-hand movements. These findings improve our understanding of the neural mechanism underlying motor preparation from the perspective of the whole-brain network.

Acknowledgments

This research was supported by the Technology Project of Henan Province (no. 202102310210), the Key Project of

Discipline Construction of Zhengzhou University (no. XKZDQY201905), the Chinese National Natural Science Foundation (no. 82001112), the Medical Science and Technology Research Project of Henan Province (no. LHGJ20190409), and the National Natural Science Foundation of China (no. 61803342).

Conflict of interest

There are no conflicts to declare.

Supporting information

Not Applicable.

References

- [1] I. Fried, P. Haggard, B. J. He, A. Schurger, *The Journal of Neuroscience*, 2017, **37**, 10842-10847, doi: 10.1523/jneurosci.2584-17.2017.
- [2] P. Haggard, *Nature Reviews Neuroscience*, 2008, **9**, 934-946, doi: 10.1038/nrn2497.
- [3] H. H. Kornhuber, L. Deecke, *Pflügers Arch Gesamte Physiol Menschen Tiere*, 1965, **10**, 1-17.
- [4] F. D. Russo, C. Incoccia, R. Formisano, U. Sabatini, P. Zoccolotti, *Journal of Neurotrauma*, 2005, **22**, 297-312, doi: 10.1089/neu.2005.22.297.
- [5] M. Berchicci, D. Spinelli, F. di Russo, *Biological Psychology*, 2016, **117**, 202-215, doi: 10.1016/j.biopsycho.2016.04.007.
- [6] M. Berchicci, G. Lucci, D. Spinelli, F. di Russo, *Frontiers in Behavioral Neuroscience*, 2015, **9**, 101, doi: 10.3389/fnbeh.2015.00101.
- [7] M. Berchicci, M. B. Pontifex, E. S. Drollette, C. Pesce, C. H. Hillman, F. di Russo, *Neuroscience*, 2015, **298**, 211-219, doi: 10.1016/j.neuroscience.2015.04.028.
- [8] F. di Russo, G. Lucci, V. Sulpizio, M. Berchicci, D. Spinelli, S. Pitzalis, G. Galati, *NeuroImage*, 2016, **126**, 1-14, doi: 10.1016/j.neuroimage.2015.11.036.
- [9] V. Sulpizio, G. Lucci, M. Berchicci, G. Galati, S. Pitzalis, F. di Russo, *NeuroImage*, 2017, **148**, 390-402, doi: 10.1016/j.neuroimage.2017.01.009.
- [10] R. Cunnington, C. Windischberger, L. Deecke, E. Moser, *NeuroImage*, 2002, **15**, 373-385, doi: 10.1006/nimg.2001.0976.
- [11] F. di Russo, M. Berchicci, C. Bozzacchi, R. L. Perri, S. Pitzalis, D. Spinelli, *Neuroscience & Biobehavioral Reviews*, 2017, **78**, 57-81, doi: 10.1016/j.neubiorev.2017.04.019.
- [12] M. Lotze, U. Halsband, *Journal of Physiology-Paris*, 2006, **99**, 386-395, doi: 10.1016/j.jphysparis.2006.03.012.
- [13] C. Neuper, M. Wortz, G. Pfurtscheller, *Progress in Brain Research*, 2006, **159**, 211-222, doi: 10.1016/S0079-6123(06)59014-4.
- [14] K. Wang, M. Xu, Y. Wang, S. Zhang, L. Chen, D. Ming, *Journal of Neural Engineering*, 2020, **17**, 016033, doi: 10.1088/1741-2552/ab598f.
- [15] S. L. Bressler, V. Menon, *Trends in Cognitive Sciences*, 2010, **14**, 277-290, doi: 10.1016/j.tics.2010.04.004.
- [16] T. P. Meehan, S. L. Bressler, *Neuroscience & Biobehavioral Reviews*, 2012, **36**, 2232-2247, doi:

- 10.1016/j.neubiorev.2012.08.002.
- [17] M. D. Fox, A. Z. Snyder, J. L. Vincent, M. Corbetta, D. C. van Essen, M. E. Raichle, *Proceedings of the National Academy of Sciences of the United States of America*, 2005, **102**, 9673-9678, doi: 10.1073/pnas.0504136102.
- [18] M. D. Fox, M. E. Raichle, *Nature Reviews Neuroscience*, 2007, **8**, 700-711, doi: 10.1038/nrn2201.
- [19] C. M. Michel, T. Koenig, *NeuroImage*, 2018, **180**, 577-593, doi: 10.1016/j.neuroimage.2017.11.062.
- [20] F. Schlegel, D. Lehmann, P. L. Faber, P. Milz, L. R. R. Gianotti, *Brain Topography*, 2012, **25**, 20-26, doi: 10.1007/s10548-011-0189-7.
- [21] C. Chu, X. Wang, L. Cai, L. Zhang, J. Wang, C. Liu, X. Zhu, *NeuroImage: Clinical*, 2020, **25**, 102132, doi: 10.1016/j.nicl.2019.102132.
- [22] J. Britz, D. van de Ville, C. M. Michel, *NeuroImage*, 2010, **52**, 1162-1170, doi: 10.1016/j.neuroimage.2010.02.052.
- [23] F. Musso, J. Brinkmeyer, A. Mobascher, T. Warbrick, G. Winterer, *NeuroImage*, 2010, **52**, 1149-1161, doi: 10.1016/j.neuroimage.2010.01.093.
- [24] H. Yuan, V. Zotev, R. Phillips, W. C. Drevets, J. Bodurka, *NeuroImage*, 2012, **60**, 2062-2072, doi: 10.1016/j.neuroimage.2012.02.031.
- [25] K. Nishida, Y. Morishima, M. Yoshimura, T. Isotani, S. Irisawa, K. Jann, T. Dierks, W. Strik, T. Kinoshita, T. Koenig, *Clinical Neurophysiology*, 2013, **124**, 1106-1114, doi: 10.1016/j.clinph.2013.01.005.
- [26] C. Andreou, P. L. Faber, G. Leicht, D. Schoettle, N. Polomac, I. L. Hanganu-Opatz, D. Lehmann, C. Mulert, *Schizophrenia Research*, 2014, **152**, 513-520, doi: 10.1016/j.schres.2013.12.008.
- [27] P. Gui, Y. Jiang, D. Zang, Z. Qi, J. Tan, H. Tanigawa, J. Jiang, Y. Wen, L. Xu, J. Zhao, Y. Mao, M.-M. Poo, N. Ding, S. Dehaene, X. Wu, L. Wang, *Nature Neuroscience*, 2020, **23**, 761-770, doi: 10.1038/s41593-020-0639-1.
- [28] M. Grieder, T. Koenig, T. Kinoshita, K. Utsunomiya, L.-O. Wahlund, T. Dierks, K. Nishida, *Clinical Neurophysiology*, 2016, **127**, 2175-2181, doi: 10.1016/j.clinph.2016.01.025.
- [29] M. Gschwind, M. Hardmeier, D. van de Ville, M. I. Tomescu, I.-K. Penner, Y. Naegelin, P. Fuhr, C. M. Michel, M. Seeck, *NeuroImage: Clinical*, 2016, **12**, 466-477, doi: 10.1016/j.nicl.2016.08.008.
- [30] F. Gao, H. Jia, X. Wu, D. Yu, Y. Feng, *Brain Topography*, 2017, **30**, 233-244, doi: 10.1007/s10548-016-0520-4.
- [31] S. Schmidt, H.-G. Jo, M. Wittmann, T. Hinterberger, *Neuroscience & Biobehavioral Reviews*, 2016, **68**, 639-650, doi: 10.1016/j.neubiorev.2016.06.023.
- [32] A. Schurger, P. Hu, J. Pak, A. L. Roskies, *Trends in Cognitive Sciences*, 2021, **25**, 558-570, doi: 10.1016/j.tics.2021.04.001.
- [33] Y. Hu, L. Zhang, M. Chen, X. Li, L. Shi, *Frontiers in Neuroscience*, 2017, **11**, 683, doi: 10.3389/fnins.2017.00683.
- [34] T.-P. Jung, S. Makeig, M. Westerfield, J. Townsend, E. Courchesne, T. J. Sejnowski, *Clinical Neurophysiology*, 2000, **111**, 1745-1758, doi: 10.1016/s1388-2457(00)00386-2.
- [35] P. L. Nunez, B. M. Wingeier, R. B. Silberstein, *Human Brain Mapping*, 2001, **13**, 125-164, doi: 10.1002/hbm.1030.
- [36] A. T. Poulsen, A. Pedroni, N. Langer, L. K. Hansen, *bioRxiv*, 2018, **1**, 1-30, doi: 10.1101/289850
- [37] Y. Benjamini, Y. Hochberg, *Journal of the Royal Statistical Society: Series B (Methodological)*, 1995, **57**, 289-300, doi: 10.1111/j.2517-6161.1995.tb02031.x.
- [38] M. M. Murray, D. Brunet, C. M. Michel, *Brain Topography*, 2008, **20**, 249-264, doi: 10.1007/s10548-008-0054-5.
- [39] B. A. Seitzman, M. Abell, S. C. Bartley, M. A. Erickson, A. R. Bolbecker, W. P. Hetrick, *NeuroImage*, 2017, **146**, 533-543, doi: 10.1016/j.neuroimage.2016.10.002.
- [40] A. Khanna, A. Pascual-Leone, C. M. Michel, F. Farzan, *Neuroscience & Biobehavioral Reviews*, 2015, **49**, 105-113, doi: 10.1016/j.neubiorev.2014.12.010.
- [41] E. Travers, P. Haggard, *European Journal of Neuroscience*, 2021, **53**, 1533-1544, doi: 10.1111/ejn.15063.
- [42] R. J. Kobler, E. Kolesnichenko, A. I. Sburlea, G. R. Müller-Putz, *NeuroImage*, 2020, **220**, 117076, doi: 10.1016/j.neuroimage.2020.117076.
- [43] G. Pfurtscheller, F. H. Lopes da Silva, *Clinical Neurophysiology*, 1999, **110**, 1842-1857, doi: 10.1016/s1388-2457(99)00141-8.
- [44] V. Menon, L. Q. Uddin, *Brain Structure and Function*, 2010, **214**, 655-667, doi: 10.1007/s00429-010-0262-0.
- [45] S. K. Peters, K. Dunlop, J. Downar, *Frontiers in Systems Neuroscience*, 2016, **10**, 104, doi: 10.3389/fnsys.2016.00104.
- [46] V. T. Nguyen, M. Breakspear, R. Cunnington, *The Journal of Neuroscience*, 2014, **34**, 16397-16407, doi: 10.1523/jneurosci.2571-14.2014.
- [47] M. Dhamala, G. Pagnoni, K. Wiesenfeld, C. F. Zink, M. Martin, G. S. Berns, *NeuroImage*, 2003, **20**, 918-926, doi: 10.1016/s1053-8119(03)00304-5.
- [48] M. Sabaté, B. González, M. Rodríguez, *Neuropsychologia*, 2004, **42**, 1041-1049, doi: 10.1016/j.neuropsychologia.2003.12.015.

Author Information



Lipeng Zhang was born in Luoyang, Henan, China in 1989. In 2013, he received the B.S degree in Automation from Henan University of Urban Construction. In 2016, he received the M.S degree in Navigation, guidance and control from Zhengzhou University. From 2016 to 2018, he was a Research Assistant in the Department of Automation, Tsinghua University. Since 2018, he is pursuing his Ph.D degree in Zhengzhou University. His research interests include brain-computer interface and the brain mechanism motor execution.



Tongda Shen is currently a student in Tandon School of Engineering, New York University. From 2019 to 2021, he got an internship at Henan Key Laboratory of Brain Science and Brain-Computer Interface Technology and participated in the research of the rehab training device.



Rui Zhang was born in Hebi, Henan province 1987. He received the Ph.D. degree in Biomedical Engineering from the School of Life Science and Technology, University of Electronic Science and Technology of China in 2015. He is currently an Associate Professor at the School of Electrical Engineering, Zhengzhou University, P. R. China. His research interests include the brain-computer interface, EEG signal processing, neurorehabilitation and brain network analysis, etc.



Yuxia Hu received the B.S. degree in automation from the Zhengzhou University of Technology, Zhengzhou, China, in 1999, and the M.S. degree in electrical theory and new technology from Zhengzhou University, Zhengzhou, in 2005, where she has been with the School of Electrical Engineering, since 1999. She received the Ph.D. degree in Control Science and Engineering from the School of Electrical Engineering, Zhengzhou University in 2019. Her research interests include pattern recognition and biomedical engineering.

Publisher's Note: Engineered Science Publisher remains neutral with regard to jurisdictional claims in published maps and institutional affiliations.